Imaging Nanoclusters in 3D

DOI: 10.1002/anie.201300238

Three-Dimensional Structural Analysis of MgO-Supported Osmium Clusters by Electron Microscopy with Single-Atom Sensitivity**

*Ceren Aydin, Apoorva Kulkarni, Miaofang Chi, Nigel D. Browning, and Bruce C. Gates**

Supported metals are a widely applied class of industrial catalyst,[1] with properties depending on the size, shape, and structure of the metal species.[2,3] The sensitivity of the catalytic properties to the structure is maximized when the structures are smallest[4] and the interactions of the metal with the support maximized.[5] Consequently, attention has increasingly been focused on metal species in the size range between single-metal-atom (mononuclear) metal complexes[6] and clusters[7] that incorporate less than about 10 metal atoms. Work on such catalysts is now emerging from industrial laboratories, especially those concerned with supported platinum for hydrocarbon conversions.[8,9] Understanding of the properties of such highly dispersed metals is benefiting especially from the application of atomic-resolution scanning transmission electron microscopy (STEM).[10] Recent reports, including those from industry,[11] illustrate the power of this technique, especially when used in concert with spectroscopic methods.[12] Important next steps are determination of the nuclearities and three-dimensional structures of supported metal clusters present in mixtures typical of industrial catalysts.

Three-dimensional structures can in prospect be determined by tomographic imaging techniques, but the methods require long sample exposures for imaging at multiple angles,[13] and beam-sensitive samples do not survive. Consequently, atomic-resolution tomography of small supported metal clusters has not yet been achieved with this technique.

To acquire such information about highly dispersed supported metals, we took a different approach, pushing the limits of imaging by aberration-corrected STEM, characterizing small three-dimensional metal clusters by their two-dimensional projections. Thus, we extracted 3D structures from atomic-resolution images acquired with short dwell times to minimize the influence of the electron beam on the samples—without significantly compromising the signal-to-noise ratios. We illustrate the approach with a characterization of MgO-supported osmium clusters having nuclearities of 10 and less in mixtures of planar (2D) and 3D structures.

The metal was chosen to be osmium because oxide-supported osmium carbonyl clusters are catalysts for reactions including alkene isomerization[14] and hydrogenation,[15] carbon monoxide hydrogenation,[16] and alkane hydrogenolysis.[17] Osmium offers the further advantages of being a metal that is a) heavy, offering high contrast with supports consisting of light atoms in STEM imaging, b) synthesizable in the form of carbonyl clusters of various nuclearities, and c) relatively stable in the electron beam.[18] These clusters have been synthesized as osmium carbonylate ions in basic solutions and on basic supports.[19]

MgO was chosen as the support because it is a) basic, facilitating the cluster syntheses, b) composed of light atoms, for contrast with osmium in STEM imaging, and c) present in the high-area powder form as highly crystalline particles that are stable in the electron beam.

In the syntheses, $[Os_3(CO)_{12}]$ reacted with MgO powder (surface area 115 $m^2 g^{-1}$) in a *n*-pentane slurry to give supported clusters that are well approximated as $[Os_3(CO)_{11}]^{2-}$.[20,21] The supported clusters were exposed to flowing helium at 548 K and 1 bar for 2 h to form supported mononuclear $[Os(CO)_2]$ complexes;[22] these were treated in flowing CO at 548 K and 1 bar for 4 h to give $[Os_{10}C(CO)_{24}]^{2-}$,[19] among other clusters, on the MgO surface.

The samples were imaged with aberration-corrected STEM and characterized by infrared (IR) and extended X-ray absorption fine structure (EXAFS) spectroscopies (Figures S2–S4 in the Supporting Information). A major goal was to determine the structures of the metal frames and compare them with those of individual osmium cluster carbonyl compounds characterized in the crystalline state by X-ray diffraction crystallography (Figure S1). The atomic resolution images of the cluster metal frames provide satisfying agreement with the structures of known compounds.

The observations of a family of osmium carbonyl clusters in the sample agree with the results of Lamb et al.,[19] who reported the surface-mediated synthesis of osmium carbonyl

[*] C. Aydin, A. Kulkarni, Prof. B. C. Gates
Department of Chemical Engineering and Materials Science
University of California
One Shields Avenue, Davis, CA 95616 (USA)
E-mail: bcgates@ucdavis.edu
Homepage: http://www.chms.ucdavis.edu/research/web/catalysis
M. Chi
Materials Science & Technology Division
Oak Ridge National Laboratory, Oak Ridge, TN 37830 (USA)
Prof. N. D. Browning
Fundamental and Computational Sciences Division
Pacific Northwest National Laboratory
902 Battelle Boulevard, Richland, WA 99352 (USA)

[**] This work was supported by the Department of Energy (DOE), grants DE-SC0005822 and DE-FG02-03ER46057 (C.A.) and the University of California Lab Fee Program. The electron microscopy experiments were performed at the Oak Ridge National Laboratory Shared Research Equipment (ShaRE) User Facility, which is supported by the Division of Scientific User Facilities, DOE Office of Science, Basic Energy Sciences. We acknowledge beam time and support of the DOE Office of Science, Materials Sciences, for its role in the operation and development of beamlines 4-1 and 10-2 at the Stanford Synchrotron Radiation Lightsource.

Supporting information for this article is available on the WWW under http://dx.doi.org/10.1002/anie.201300238.

cluster anions with various nuclearities on MgO by the procedure that we used. The formation of the supported osmium carbonyl clusters involves break-up of the triosmium frame of the precursor to give mononuclear species, which in the presence of added CO are then converted into tetraosmium, pentaosmium, and decaosmium carbonyl clusters. Lamb et al.[19] reported a yield of decaosmium clusters of as much as approximately 65%.

A comparison of the Fourier transforms of the EXAFS data[23] characterizing the sample after various treatments (Figure S4) shows the gradual formation of larger clusters from the mononuclear osmium species; the magnitude of the EXAFS (χ) function at a distance of ca. 2.6 Å (not corrected for phase shifts), assigned to Os–Os bonds in the nearest metal–metal coordination shell, correlates with the number of Os atoms at that interatomic distance. As triosmium clusters fragmented to give mononuclear complexes, the intensity contribution of the scattering decreased (the first-shell Os–Os coordination number (CN) decreased from approximately 2 to essentially 0).[22] These complexes were subsequently converted to increasingly large clusters (a mixture with a majority being Os_5 species,[19] corresponding to a CN of approximately 4, and ultimately to a mixture of Os_n species where n is 1, 3, 4, 5, and 10 for the species we could identify).

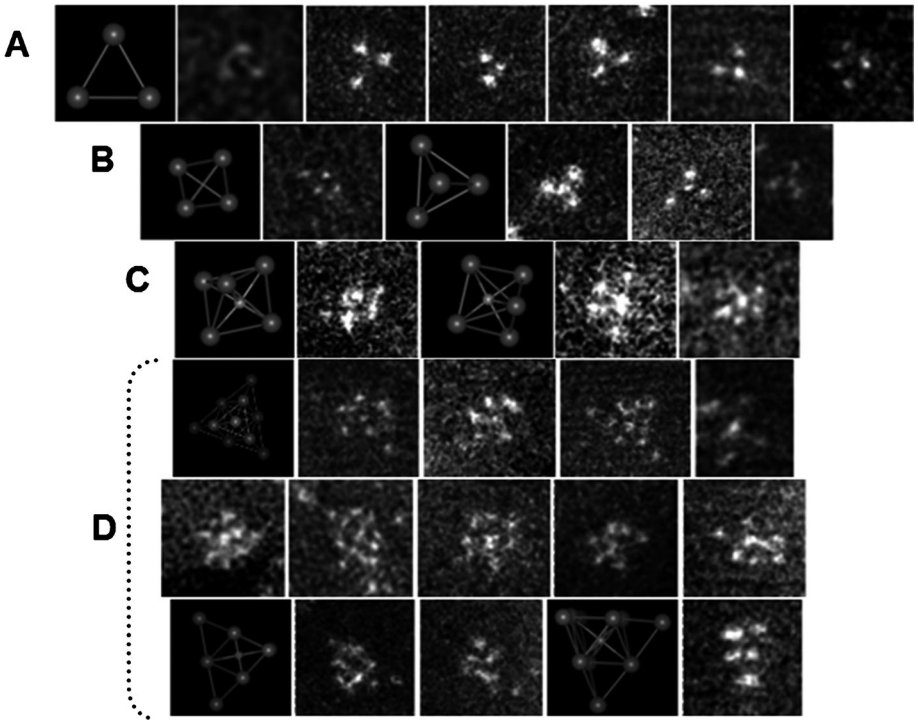

Figure 1. Crystallographic models of osmium clusters and corresponding images of MgO-supported osmium clusters. A) Os_3 framework in $[Os_3(CO)_{11}]^{2-}$ and images of Os_3 clusters, B) Os_4 framework in $[H_3Os_4(CO)_{12}]^-$ and images of Os_4 clusters, C) Os_5 framework in $[Os_5C(CO)_{14}]^{2-}$ and images of Os_5 clusters, D) Os_{10} framework in $[Os_{10}C(CO)_{24}]^{2-}$ and images of Os_{10} clusters. Images are of sample treated in flowing helium at 548 K and 1 bar for 2 h followed by flowing CO at 548 K and 1 bar for 4 h, as described in the text (the scale bars are shown in the corresponding images in the Supporting Information, Figures S5–S18).

The ν_{CO} IR spectra (Figure S2) of the samples match those reported.[24] In the formation of the mixtures, some of the osmium species must have been intermediates in the formation of others, but the X-ray absorption near edge spectra (XANES) characterizing the formation of the mixtures are not characterized by isosbestic points (Figure S3), showing that the transformations were not stoichiometrically simple.

We stress that, because of the complexity of the samples, the IR and EXAFS spectra are not sufficient to resolve the mixtures. But the STEM images (Figure 1 and Figures S5–S18) now provide the desired resolution. They show single, isolated Os atoms as well as Os_3, Os_4, Os_5, and Os_{10} clusters. Among the osmium clusters, those with atomically resolved metal frames were identified by comparisons of projections in the images with models based on crystallographic data characterizing the corresponding osmium cluster carbonyls.[25] However, some clusters were not aligned in projections that allowed detailed structural analysis; thus, we cannot rule out the possibility that some clusters other than the ones identified were present.

The STEM images shown in Figure 1 A–D were smoothed for better visualization, but all the analyses were performed with the original images (shown in the Supporting Information). Intensity analyses were performed to determine the number of Os atoms in each cluster. The intensity variations within the images of the clusters were analyzed by investigating the total intensity across the atoms of the osmium-containing species, and intensity profiles were drawn. The intensity contribution from the MgO support was subtracted as background from the total intensity, because the support thickness (and therefore its intensity contribution) was not the same in each region of the sample. The intensity of a single Os atom in the region close to the cluster of interest was measured in each image as a reference, and the same background subtraction technique was applied in each case. The background-subtracted intensity of each column of Os atoms in a cluster and the background-subtracted intensity of a single Os atom in the vicinity were then compared. Standard deviations in intensity measurements were calculated on the basis of an image of a sample incorporating solely mononuclear osmium species on MgO.[22]

The analysis method is illustrated in Figure 2. The number of Os atoms in each cluster was established by comparison of the intensities with respect to that of the single reference Os atom. In the analysis of the cluster shown in Figure 2 A, for example, we inferred that it contained 10 Os atoms, as the

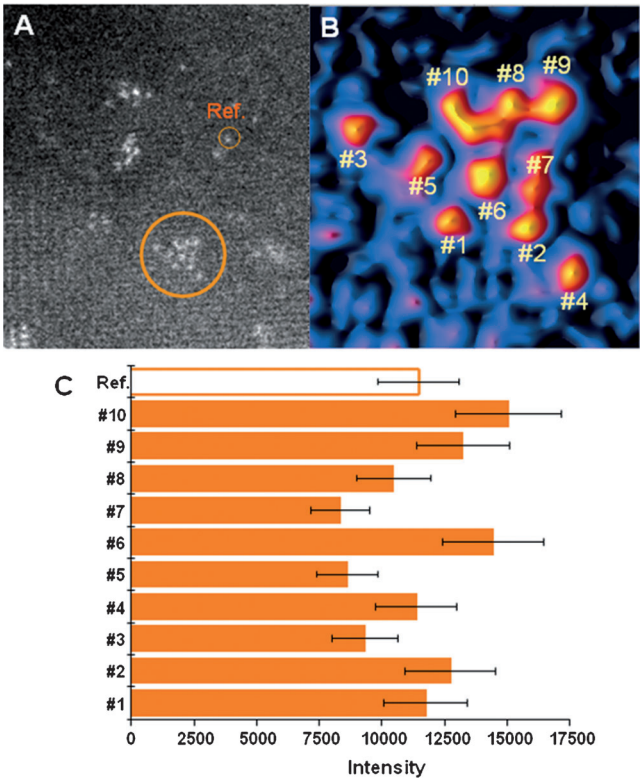

Figure 2. A) Z-contrast HAADF-STEM image of sample incorporating osmium carbonyl clusters formed by treatment of fragmented triosmium clusters on MgO powder in flowing CO. B) Intensity surface plot of the cluster (Os_{10}), shown in the circled region in image (A). C) Intensity measurements of each Os atom in the Os_{10} cluster compared with the single Os atom as a reference. The error bars represent the standard deviations in intensity measurements. Although extreme care was taken, some atoms in the osmium clusters were observed to move during imaging, causing a streak of intensity around the atom, as illustrated for the Os atom labeled #10 in this cluster. Artifacts such as these including migration of metal atoms or small clusters occur under these imaging conditions as reported elsewhere.[29,30]

projection of the cluster core matches that of the crystallographically determined frame of $[Os_{10}C(CO)_{24}]^{2-}$ (Figure S1D).

Os–Os distances in the supported clusters were estimated by analysis of the images and compared with crystallographic data characterizing the metal frames of the clusters shown in Figure S1. The average Os–Os distance in the supported Os_4 clusters was found to be 2.83 ± 0.02 Å on the basis of the projection shown in Figure 1B; the corresponding crystallographic value for $[H_3Os_4(CO)_{12}]^-$[26] is 2.88 Å. The average bond angle between Os atoms in the supported Os_4 clusters was calculated to be 61° on the basis of the distances between the top Os atom and the Os atoms in the triangular base in the projection shown in Figure 1B. This result matches the crystallographically value (60°) for $[H_3Os_4(CO)_{12}]^-$.[26] The average Os–Os bond length in the supported Os_5 clusters, determined from the images (Figure 1C), was 2.85 ± 0.02 Å, and the crystallographic value for $[Os_5C(CO)_{14}]^{2-}$[27] is 2.87 Å.

Os–Os distances in the Os_{10} clusters shown in Figure 1D were measured for the projection showing top views of the clusters (with some of the bonds in the plane of the image). The average Os–Os distance in the plane was found to be 2.77 ± 0.02 Å, with the average Os–Os distance adjusted for the angle of projection being 2.86 ± 0.02 Å. The corresponding crystallographic averages[28] for $[Os_{10}C(CO)_{24}]^{2-}$ are 2.80 and 2.90 Å.

We infer that the differences in the bond lengths and angles characterizing the supported clusters and the pure-compound analogues are evidence of distortion of the clusters interacting with the support—the distortion is evidenced by the shifts of the ν_{CO} bands (Figure S2) relative to those of the compounds in solution.[19] Further conclusions about the metal–support interface were precluded because the images do not show any discernible crystallographic orientations of the MgO.

In summary, the results presented here show how atomic-resolution STEM can be used to determine the sizes, shapes, and nuclearities of individual metal clusters on supports, even those in complex mixtures. The results provide unprecedented quantitative, atomic-resolution structures of supported metals and point the way to exact characterizations of highly nonuniform industrial catalysts, as well as to applications of electron microscopy for characterization of changes in catalyst structures influenced by reactive atmospheres.

Experimental Section

The sample was prepared and handled with standard techniques to exclude moisture and air. MgO-supported triosmium carbonyl clusters were prepared by the reaction of $[Os_3(CO)_{12}]$ (Strem, 99%) with calcined MgO (EM Science) slurried in dried *n*-pentane (Fisher, HPLC grade) under argon, with the slurry initially at ice temperature. After stirring of the slurry for 1 day at room temperature, the solvent was removed by evacuation. The resultant solid sample contained 2.0 wt% Os. In the first treatment step, the supported clusters were exposed to flowing helium at 548 K and 1 bar for 2 h, followed by treatment in flowing CO at 548 K and 1 bar for 4 h. The initial sample was light yellow in color, and after the second treatment, it turned dark brown. Details are given in the Supporting Information.

The samples were transported from Davis to Oak Ridge National Laboratory (ORNL), where each sample was mounted on a sample holder in an argon-filled glovebag, which had been purged with argon. The sample was transferred to the microscope under a blanket of flowing argon, with an air exposure of < 2 s. Samples were imaged with high-angle annular dark-field STEM. The microscope was an aberration-corrected FEI Titan 80/300S; the convergence angle was 30 mrad and the HAADF collection inner angle 100 mrad. The electron beam energy, current, and probe size were 200 kV, ≈ 10 pA, and ≈ 0.9 Å, respectively. To minimize artifacts in the images caused by beam damage, the microscope was aligned for one region of the sample, and then the beam was shifted to a neighboring region for quick image acquisition: 4 s for a 1024×1024 pixel size. This method ensured minimal exposure of the imaged area to the electron beam. Details are provided in the Supporting Information.

Received: January 11, 2013
Published online: April 16, 2013

Keywords: clusters · electron microscopy · osmium · supported catalysts

[1] C. H. Bartholomew, R. J. Farrauto, *Fundamentals of Industrial Catalytic Processes*, Wiley, Hoboken, **2006**, p. 62.
[2] Y.-H. Chin, E. Iglesia, *J. Phys. Chem. C* **2011**, *115*, 17845 – 17855.
[3] J. E. Mondloch, E. Bayram, R. G. Finke, *J. Mol. Catal. A* **2012**, *355*, 1 – 38.
[4] T. Takei, T. Akita, I. Nakamura, T. Fujitani, M. Okumura, K. Okazaki, J. Huang, T. Ishida, M. Haruta, *Adv. Catal.* **2012**, *55*, 1 – 126.
[5] G. N. Vayssilov, Y. Lykhach, A. Migani, T. Staudt, G. P. Petrova, N. Tsud, T. Skála, A. Bruix, F. Illas, K. C. Prince, V. Matolín, K. M. Neyman, J. Libuda, *Nat. Mater.* **2011**, *10*, 310 – 315.
[6] Y. Zhai, D. Pierre, R. Si, W. Deng, P. Ferrin, A. U. Nilekar, G. Peng, J. A. Herron, D. C. Bell, H. Saltsburg, M. Mavrikakis, M. Flytzani-Stephanopoulos, *Science* **2010**, *329*, 1633 – 1636.
[7] A. Okrut, O. Gazit, N. de Silva, R. Nichiporuk, A. Solovyov, A. Katz, *Dalton Trans.* **2012**, *41*, 2091 – 2099.
[8] C. Mager-Maury, C. Chizallet, P. Sautet, P. Raybaud, *ACS Catal.* **2012**, *2*, 1346 – 1357.
[9] S. A. Bradley, W. Sinkler, D. A. Blom, W. Bigelow, P. M. Voyles, L. F. Allard, *Catal. Lett.* **2012**, *142*, 176 – 182.
[10] A. A. Herzing, C. J. Kiely, A. F. Carley, P. Landon, G. J. Hutchings, *Science* **2008**, *321*, 1331 – 1335.
[11] L. P. Hansen, Q. M. Ramasse, C. Kisielowski, M. Brorson, E. Johnson, H. Topsøe, S. Helveg, *Angew. Chem.* **2011**, *123*, 10335 – 10338; *Angew. Chem. Int. Ed.* **2011**, *50*, 10153 – 10156.
[12] S. R. Bare, S. D. Kelly, F. D. Vila, E. Boldingh, E. Karapetrova, J. Kas, G. E. Mickelson, F. S. Modica, N. Yang, J. J. Rehr, *J. Phys. Chem. C* **2011**, *115*, 5740 – 5755.
[13] I. Arslan, J. C. Walmsley, E. Rytter, E. Bergene, P. A. Midgley, *J. Am. Chem. Soc.* **2008**, *130*, 5716 – 5719.
[14] X.-J. Li, B. C. Gates, *J. Catal.* **1983**, *84*, 55 – 64.
[15] M. Deeba, B. C. Gates, *J. Catal.* **1981**, *67*, 303 – 307.
[16] N. Bungane, C. Welker, E. van Steen, J. Moss, M. Claeys, *Z. Naturforsch. B* **2008**, *63*, 289 – 292.
[17] E. I. Ko, R. L. Garten, *J. Catal.* **1981**, *68*, 233 – 236.
[18] V. Ortalan, A. Uzun, B. C. Gates, N. D. Browning, *Nat. Nanotechnol.* **2010**, *5*, 843 – 847.
[19] H. H. Lamb, A. S. Fung, P. A. Tooley, J. Puga, T. R. Krause, M. J. Kelley, B. C. Gates, *J. Am. Chem. Soc.* **1989**, *111*, 8367 – 8373.
[20] R. Psaro, C. Dossi, R. Ugo, *J. Mol. Catal.* **1983**, *21*, 331 – 351.
[21] V. A. Bhirud, H. Iddir, N. D. Browning, B. C. Gates, *J. Phys. Chem. B* **2005**, *109*, 12738 – 12741.
[22] C. Aydin, A. Kulkarni, M. Chi, N. D. Browning, B. C. Gates, *J. Phys. Chem. Lett.* **2012**, *3*, 1865 – 1871.
[23] We were not able to determine a meaningful fit of the EXAFS data using the methods described elsewhere,[22] because, as evidenced by the STEM images, the samples consisted of mixtures of osmium species with a range of structures. EXAFS spectroscopy gives information averaged over the whole sample and lacks the sensitivity for resolution of mixtures such as ours.
[24] H. H. Lamb, B. C. Gates, *J. Phys. Chem.* **1992**, *96*, 1099 – 1105; B. C. Gates, H. H. Lamb, *J. Mol. Catal.* **1989**, *52*, 1 – 18.
[25] B. F. G. Johnson, J. Lewis, W. J. H. Nelson, J. N. Nicholls, M. D. Vargas, *J. Organomet. Chem.* **1983**, *249*, 255 – 272.
[26] Y.-Y. Choi, W.-T. Wong, *J. Organomet. Chem.* **1999**, *573*, 189 – 201.
[27] B. F. G. Johnson, J. Lewis, W. J. H. Nelson, J. N. Nicholls, J. Puga, P. R. Raithby, M. J. Rosales, M. Schröder, M. D. Vargas, *J. Chem. Soc. Dalton Trans.* **1983**, 2447 – 2457.
[28] P. F. Jackson, B. F. G. Johnson, J. Lewis, W. J. H. Nelson, M. McPartlin, *J. Chem. Soc. Dalton Trans.* **1982**, 2099 – 2107.
[29] C. Aydin, J. Lu, A. J. Liang, C. Y. Chen, N. D. Browning, B. C. Gates, *Nano Lett.* **2011**, *11*, 5537 – 5541.
[30] C. Aydin, J. Lu, N. D. Browning, B. C. Gates, *Angew. Chem.* **2012**, *124*, 6031 – 6036; *Angew. Chem. Int. Ed.* **2012**, *51*, 5929 – 5934.

